



Amer Alizadeh^{1,2} 
Moran Wang¹ 

¹Department of Engineering
Mechanics, Tsinghua
University, Beijing, P. R. China

²Department of Mechanical
Engineering, School of
Engineering, The University of
Tokyo, Tokyo, Japan

Received September 21, 2019

Revised March 13, 2020

Accepted March 13, 2020

Research Article

Temperature effects on electrical double layer at solid-aqueous solution interface

Despite the significant influence of solution temperature on the structure of electrical double layer, the lack of theoretical model intercepts us to explain and predict the interesting experimental observations. In this work, we study the structure of electrical double layer as a function of thermochemical properties of the solution by proposing a phenomenological temperature dependent surface complexation model. We found that by introducing a buffer layer between the diffuse layer and stern layer, one can explain the sensitivity of zeta potential to temperature for different bulk ion concentrations. Calculation of the electrical conductance as function of thermochemical properties of solution reveals the electrical conductance not only is a function of bulk ion concentration and channel height but also the solution temperature. The present work model can provide deep understanding of micro- and nanofluidic devices functionality at different temperatures.

Keywords:

Electrical double layer / Surface complexation model / Temperature effects / Zeta potential
DOI 10.1002/elps.201900354

1 Introduction

The formation of the polarized solution layer, so-called electrical double layer (EDL), at the vicinity of chemically reactive solid surfaces has been a subject of debate for decades [1,2]. This layer is responsible for diverse interesting multiphysicochemical transport phenomena associated with natural or artificial micro- and nanoscale media [3-8]. The electrochemical properties of the EDL can be manipulated by means of several parameters, such as ion concentration, solution pH, metal-oxide surface site density, chemical equilibrium constants [9,10], and solution temperature [11-13], where the former parameters have been extensively studied through large body of literature [1,14-16]. Quite surprisingly, temperature effects on structure of EDL at the vicinity of a chemically active solid surface have drawn less attention or ignored to expedite the analysis while it emerges as a determinative factor in many micro- and nanofluidics applications [17-27]. Several experimental works have shown that the zeta potential of solid-aqueous interface is not only a function of bulk ion concentration and solution pH but also solution temperature [13,26,28-32]. However, a few studies have tried to investigate the temperature dependent zeta potential from theoretical point of view. Revil and co-workers [12] proposed a simple model based on two as-

sumptions: neglecting (I) the impact of hydronium H^+ and hydroxyl OH^- ions, and (II) direct adsorption of cations K^+ or Na^+ to the silica surface. In their model, the slope of zeta potential versus the logarithm of salinity is solely a function of temperature. Later, though, Revil et al. [33] discussed the temperature effects on the streaming potentials, however, the detailed insight into the temperature effects on the EDL was not studied. The least understanding of temperature effects on the EDL brings crucial necessity to propose a comprehensive model which considers the detailed of thermochemical properties of solid-aqueous interface on the EDL structure. This work aims to investigate the effects of solution temperature on the structure of EDL for different bulk ion concentration. We, first, show that the well-known electrical triple layer (ETL) model fails to predict the measured temperature dependent zeta potentials [26] even though the temperature dependent thermochemical properties are introduced to this model. To overcome the drawback of ETL model in modeling the temperature effects on the structure of EDL, we employ a recently developed electrical quad-layer model (EQL) at which a new layer, so-called buffer layer (BL), between outer-Helmholtz plane (OHP) and shear plane (zeta potential plane [ZP]) has been introduced [34]. We found that the EQL model, as a comprehensive model, could explain the electrical conductance behavior of very narrow nanochannels as well as larger size channels [35]. In the present work model, we propose that EQL model and the flexibility of the buffer layer will let us describe the interesting behavior of the solid-liquid surface charge under solution temperature variation. Finally, we simply obtain the electrical conductance of two nanochannel

Correspondence: Professor Moran Wang, Department of Engineering Mechanics, Tsinghua University, Beijing 100084, P. R. China.

Email: mrwang@tsinghua.edu.cn

Abbreviations: BL, buffer layer; DL, diffuse layer; EDL, electrical double layer; EQL, electrical quad-layer; ETL, electrical triple layer; IHP, inner-Helmholtz plane; OHL, outer-Helmholtz layer; OHP, outer-Helmholtz plane; ZP, zeta potential plane

Color online: See article online to view Figs. 1–3 in color.

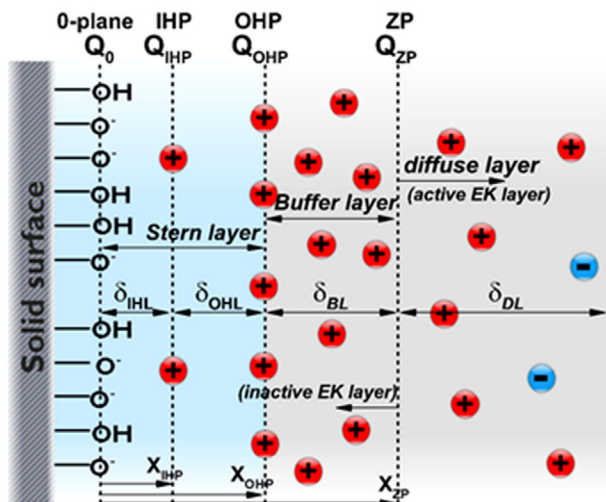


Figure 1. The configuration of the developed EQL model with a flexible buffer layer (FBL). The BL represents the distance from outer-Helmholtz plane (OHP) to zeta potential plane (ZP). The diffuse layer (DL) starts from the ZP to bulk solution. The four layers, inner-Helmholtz layer (IHL), outer-Helmholtz layer (OHL), BL, and DL postulate three series differential capacitors.

heights as function of bulk ion concentration and solution temperature.

2 Methods

2.1 Temperature dependent surface complexation model

In this section, we propose the developed temperature dependent EQL model. Figure 1 depicts our EQL model which is, in fact, a modification of the ETL model [36]. Assuming the presence of BL enables us to tackle the shortcoming of the ETL model [10, 34, 36] at which the differential capacitance of the diffuse layer (DL) was attributed to the differential capacitance of the outer-Helmholtz layer (OHL). This brings a non-physical large distance between the inner-Helmholtz plane (IHP) and OHP (order of 3 nm) [37].

Naturally, the silica surface acquires electric charge due to the chemical adsorption of ions which are dissolved in solution. In a pH range of 3–9, the typical chemical reactions at silica surface are [36]



where M^+ denotes the concentration of cations and $K_{a1}^{\text{int}}, K_{a2}^{\text{int}}, K_M^{\text{int}}$ are the inert chemical equilibrium constants.

Based on the law of mass action, the reaction equilibrium constants for the chemical adsorptions are written as

$$K_{a1}^{\text{int}} = \frac{\sigma_{\text{SiOH}}}{\sigma_{\text{SiOH}_2^+}} n_{\text{b,H}^+} \exp(-\bar{\psi}_0), \quad (4)$$

$$K_{a2}^{\text{int}} = \frac{\sigma_{\text{SiO}^-}}{\sigma_{\text{SiOH}}} n_{\text{b,H}^+} \exp(-\bar{\psi}_0), \quad (5)$$

$$K_M^{\text{int}} = \frac{\sigma_{\text{SiOM}}}{\sigma_{\text{SiO}^-}} \frac{1}{n_{\text{b,M}^+}} \exp(\bar{\psi}_{\text{IHP}}), \quad (6)$$

where σ denotes the surface charge density (in C/m^2) on the 0-plane, $\bar{\psi} = \psi/V_T$ the dimensionless electric potential where $V_T = k_B T/e$ denotes the thermal voltage, and T (in K) the temperature. It is worth pointing that Eqs. (4) and (5) are written based on the assumptions for the Boltzmann distribution which are the local equilibrium, stationary state, and insignificant fluid flow along the solid-liquid interface. Considering the total number of site density as Γ^0 (in sites per nm^2), one can write the continuity equation for the surface charge density as [10, 36, 38]

$$e\Gamma^0 = \sigma_{\text{SiOH}} + \sigma_{\text{SiO}^-} + \sigma_{\text{SiOH}_2^+} + \sigma_{\text{SiOM}}. \quad (7)$$

The surface charge density at silica surface for four planes of 0, IHP, OHP, and ZP (Fig. 1) could be written as

$$Q_0 = \sigma_{\text{SiOH}_2^+} - \sigma_{\text{SiO}^-} - \sigma_{\text{SiOM}}, \quad (8)$$

$$Q_{\text{IHP}} = \sigma_{\text{SiOM}}, \quad (9)$$

$$Q_{\text{OHP}} = -\sqrt{8\epsilon_0\epsilon_r\epsilon_{\text{r,OHL}}k_B T n_{\text{s,b}}} \sinh(0.5\bar{\psi}_{\text{OHP}}) - Q_{\text{ZP}}, \quad (10)$$

$$Q_{\text{ZP}} = -\sqrt{8\epsilon_0\epsilon_r\epsilon_{\text{r,DL}}k_B T n_{\text{s,b}}} \sinh(0.5\bar{\psi}_{\text{ZP}}), \quad (11)$$

where $n_{\text{s,b}}$ is the effective bulk number density of counter ions and hydronium (in m^{-3}) which is related to the effective bulk ionic molar concentration as $n_{\text{s,b}} = 1000N_A(n_{\text{b,M}^+} + n_{\text{b,H}^+})$, where N_A denotes the Avogadro number. Regarding the surface charge on the OHP, borrowing the idea of the Grahame's equation [15], we define

$$\begin{aligned} Q_{\text{OHP}} &= \int_{x_{\text{OHP}}}^{x_{\text{ZP}}} \rho_e dx = -\epsilon_0\epsilon_r \int_{x_{\text{OHP}}}^{x_{\text{ZP}}} \frac{d}{dx} \left(\frac{d\psi}{dx} \right) dx \\ &= -\epsilon_0\epsilon_r \left. \frac{d\psi}{dx} \right|_{x_{\text{OHP}}}^{x_{\text{ZP}}}. \end{aligned} \quad (12)$$

Based on the definition of surface charge on ZP, Eq. (12) gives rise to

$$Q_{\text{OHP}} = \epsilon_0\epsilon_r \left. \frac{d\psi}{dx} \right|_{x_{\text{OHP}}} - Q_{\text{ZP}}, \quad (13)$$

where if we introduce the Grahame's equation to Eq. (13), we finally have Eq. (10).

On the other hand, the global electroneutrality in four layers leads to

$$Q_0 + Q_{\text{IHP}} + Q_{\text{OHP}} + Q_{\text{ZP}} = 0. \quad (14)$$

Considering the presence of four planes which are in series from the solid-liquid interface to the bulk solution, one can postulate three series differential capacitors

$$\psi_0 - \psi_{\text{IHP}} = \frac{Q_0}{C_{\text{IHP}}}, \quad (15)$$

$$\psi_{\text{IHP}} - \psi_{\text{OHP}} = -\frac{Q_{\text{OHP}}}{C_{\text{OHP}}}, \quad (16)$$

$$\psi_{\text{OHP}} - \psi_{\text{ZP}} = -\frac{Q_{\text{ZP}}}{C_{\text{BL}}}, \quad (17)$$

where C_{IHP} , C_{OHP} , and C_{BL} (F/m^2) are the integral differential capacities of the inner, outer parts of the Helmholtz layer, and the BL, respectively, assuming constant in the region between planes [39]. Eqs. (4) to (11) and Eqs. (14) to (17) are formed a set of nonlinear coupled equations for the EQL. In this contribution, the constant parameters for the EQL are considered based on the solution properties as $\varepsilon_{\text{r,IHL}} = 16.1717$, $\varepsilon_{\text{r,OHL}}(T) = \varepsilon_{\text{r,BL}}(T) = 305.7 \exp(-T/219.0)$ [17], $C_{\text{IHL}} = \varepsilon_0 \varepsilon_{\text{r,IHL}}/r_{\text{K}^+}$, $C_{\text{OHP}} = \varepsilon_0 \varepsilon_{\text{r,OHL}}/2r_{\text{K}^+}$ [37], where $r_{\text{K}^+} = 0.125$ (nm) denotes the Stokes radius of K^+ [10]. The EQL is a distinct surface complexation model which allows a flexible behavior for the layer between OHP and ZP. The thickness of the BL could be obtained based on the best fitting with the available experimental data [26] as

$$\delta_{\text{BL}}(T, n_b) = \alpha(n_b) \times (T - T_0) + \beta(n_b), \quad (18)$$

where $\alpha(n_b) = 10^{-9}/(9.73 \times 10^4 n_b - 1.1173) - 10^{-11}$ and $\beta(n_b) = 10^{-9}/(3.33 \times 10^3 n_b + 6.34 \times 10^{-3}) + 1.08 \times 10^{-9}$ denote the slope of BL thickness as a function of bulk ion concentration and the thickness of the BL at $T = T_0$, respectively. In Eq. (18), $T_0 = 323.15$ (K) and n_b denotes the bulk ion concentration in molar. Eventually, we have the differential capacitance of the BL as $C_{\text{BL}} = \varepsilon_0 \varepsilon_{\text{r,BL}}/\delta_{\text{BL}}$. The electrical permittivity at vacuum is $\varepsilon_0 = 8.854 \times 10^{-12}$ (C/V/m). Regarding the temperature dependent equilibrium constants, by employing the Van't Hoff equation [13], we have $K_{a2}^{\text{int}} = 10^{-6.64} \exp(-\Delta H^0/R)(1/T - 1/298.15)$, $K_M^{\text{int}} = 10^{-0.3} \exp(-\Delta H^0/R)(1/T - 1/298.15)$ [10] and $K_{a1}^{\text{int}} = 10^{2pH_{\text{PZC}} - \log(K_{a2}^{\text{int}})}$ where for silica $\text{pH}_{\text{PZC}} = 2.5$ and $\Delta H^0 = 10^3$ (J/mol) denotes the standard enthalpy change. The surface site density of the silica is $\Gamma^0 = 5$ (nm^{-2})[10,36]. To obtain the unknown parameters of the EQL model (Q_0 , Q_{IHP} , Q_{OHP} , Q_{ZP} , ψ_0 , ψ_{IHP} , ψ_{OHP} , ψ_{ZP} , σ_{SiOH} , σ_{SiO^-} , $\sigma_{\text{SiOH}_2^+}$, σ_{SiOM}), we employ Newton's method to solve the set of equations numerically.

3 Results and discussion

The temperature dependent surface complexation model has been evaluated by fitting the available measured zeta potentials [26] for different bulk ion concentration and solution temperature in Fig. 2A. We should point out that the proposed temperature dependent surface complexation model is a phenomenological model, just following the logic of pre-

vious historical models in electrokinetics, whose parameters depend on experimental data. The model can be employed to predict other EDL parameters (i.e., surface charge, differential capacitance) as a function of various temperatures and bulk ion concentrations. To justify the necessity of proposing a new temperature dependent model, it is essential to demonstrate the failure of the previous models such as ETL in prediction of the measured zeta potentials. To this end, we introduced the relevant temperature dependent parameters (i.e., reaction equilibrium constants, electrical permittivity) into ETL model and obtained the predicted zeta potential versus temperature and bulk ion concentration. The ETL modeling results (Fig. 2A) illustrate almost an independent slope from bulk ion concentration for the zeta potential with respect to temperature ($d(\partial\zeta/\partial T)/dn_b \approx 0$). In other words, the well-known surface complexation models such as ETL fails to explain the dependency of $\partial\zeta/\partial T$ on bulk ion concentration even though we introduce the temperature dependent thermochemical properties to this model.

It would be interesting to study the effects of temperature on the acquired surface charge at silica surface whereas the surface charge density plays a crucial role in ion transport [4]. Here, we consider the system is under elevated isothermal situation only in this work. Otherwise, the thermodiffusion effect or the Soret effect may play an important role on ion transport [40-44]. Figure 2B demonstrates that the acquired surface charge (σ_0) enhances by increasing the solution temperature. Moreover, it is found that for range of low to high bulk ion concentration, the surface charge density is considerably sensitive to solution temperature in contrast to zeta potential (Fig. 2A). To investigate the structure of EDL as a function of bulk ion concentration and solution temperature, Fig. 2C and D demonstrate the slope of BL's thickness with respect to temperature solution and the differential capacitance of BL and OHL, respectively. As Eq. (18) predicts, $\partial\delta_{\text{BL}}/\partial T = \alpha(n_b)$ is a function of bulk ion concentration which saturates for concentrated solutions ($n_b \rightarrow \infty \Rightarrow d(\partial\delta_{\text{BL}}/\partial T)/dn_b = 0$). Figure 2C shows that the slope of variation of BL thickness versus bulk ion concentration is positive for low bulk ion concentrations while tends to negative amounts by increasing the bulk ion concentration. In one hand, we show that the differential capacitance of the BL increases, decreases, or remains unchanged in response to solution temperature (Fig. 2C) under diverse bulk ion concentration. On other hand, the differential capacitance of the OHL is merely a function of temperature (the dashed line with symbol at Fig. 2D). Regarding the equivalent differential capacitance for SL and BL ($1/C_{\text{SL+BL}} = 1/C_{\text{SL}} + 1/C_{\text{BL}}$), Fig. 2D shows that the differential capacitance of the BL dominates which determines the behavior of $C_{\text{SL+BL}}$ as function of bulk ion concentration and solution temperature. The nonmonotonic behavior of the differential capacitance of BL in response to temperature and bulk ion concentration which is predicted by our phenomenological EDL model remains as an open question which needs deeper theoretical (molecular dynamics) and experimental (e.g., electron impedance spectroscopy) investigations.

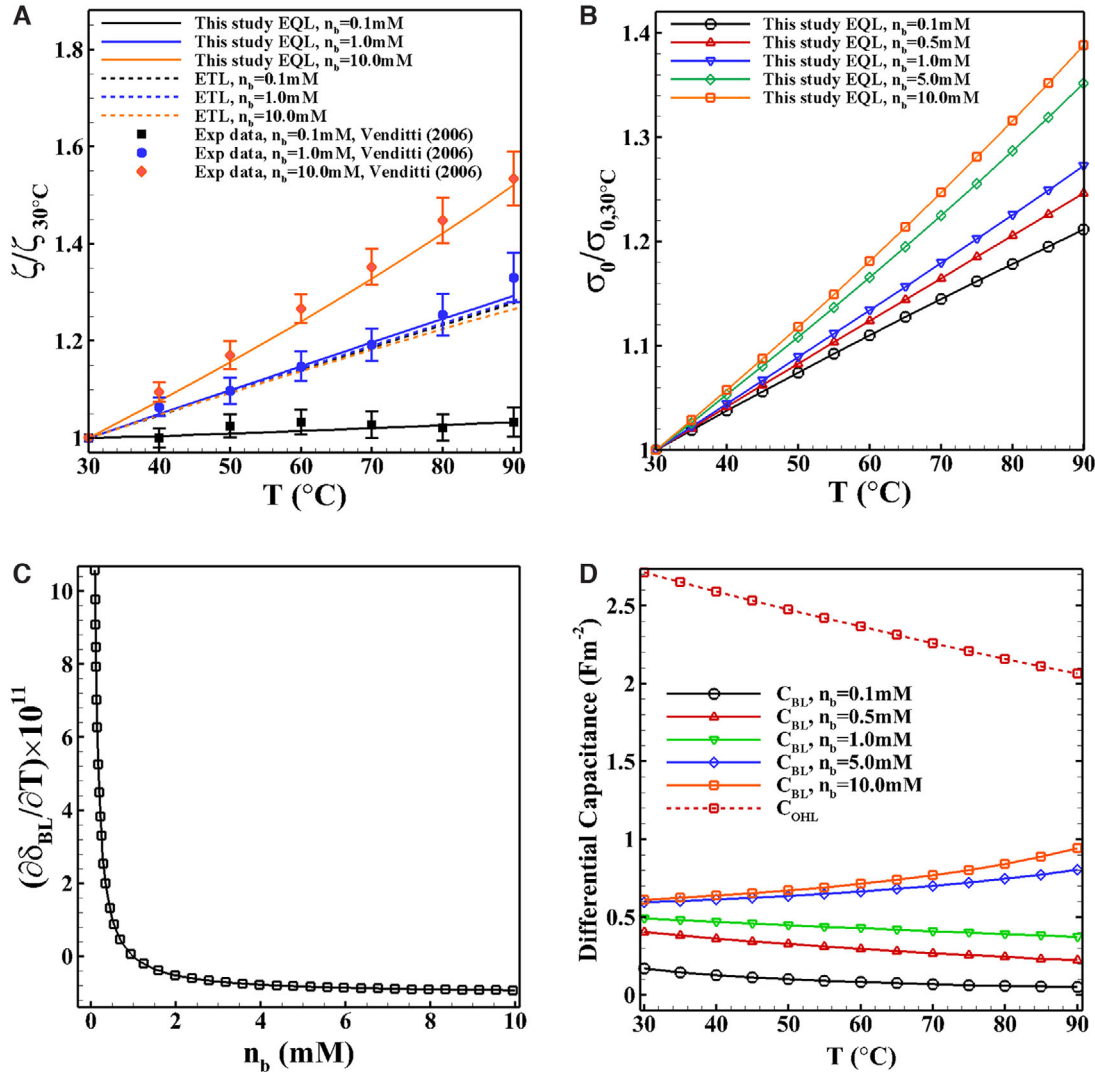


Figure 2. The normalized zeta potential and surface charge density with their corresponding amounts at $T = 30^\circ\text{C}$. (A) The predicted $\zeta/\zeta_{30^\circ\text{C}}$ versus solution temperature for different bulk ion concentration. Our modeling results with $\zeta_{30^\circ\text{C}}^{0.1\text{mM}} = -109.2$ (mV), $\zeta_{30^\circ\text{C}}^{1.0\text{mM}} = -91.3$ (mV), and $\zeta_{30^\circ\text{C}}^{10.0\text{mM}} = -58.19$ (mV) compared with the available experimental data from Venditti et al. [26] (symbols with error bars). The dashed lines demonstrate the predicted normalized zeta potential by employing the ETL model at which $\zeta_{30^\circ\text{C}}^{0.1\text{mM}} = -118.7$ (mV), $\zeta_{30^\circ\text{C}}^{1.0\text{mM}} = -84.8$ (mV), and $\zeta_{30^\circ\text{C}}^{10.0\text{mM}} = -48.84$ (mV). (B) The predicted $\sigma_0/\sigma_{0,30^\circ\text{C}}$ versus solution temperature and bulk ion concentration where $\sigma_{0,30^\circ\text{C}}^{0.1\text{mM}} = -7.9$ (mC/m²), $\sigma_{0,30^\circ\text{C}}^{1.0\text{mM}} = -15.69$ (mC/m²), $\sigma_{0,30^\circ\text{C}}^{10.0\text{mM}} = -29.5$ (mC/m²). (C) The slope of the BL thickness with respect to solution temperature versus the bulk ion concentration. (D) The differential capacitance of the BL (solid lines with symbols) and OHL (dashed line with symbol) versus solution temperature for different bulk ion concentration. The C_{OHL} is only function of temperature.

By employing our temperature dependent surface complexation model coupled with the Poisson–Boltzmann equation, we simply calculate the electrical conductance, $G \equiv I/E_p L = (eW_H/E_p L) \int_0^{H_{\text{eff}}} ((\mu_o E_p)(c^+(y) - c^-(y))) dy$ [4], of two distinct nanochannels (Fig. 3), where G , I , $E_p = 357$ (V/m), $H_{\text{eff}} = H - 2(3r_{K^+} + \delta_{\text{BL}})$, $L = 140$ (μm) and $W_H = 2$ (μm) denote the electrical conductance (in S), ionic current (in A), strength of applied external electric field, effective height of nanochannel, length and width of channel, respectively. $c^\pm(y) = n_b \exp(\mp e\psi/k_B T)$ and $\mu_o = e/6\pi r_{K^+} \eta$ denote the local concentration of cations, anions, and mobility of ions [15], respectively. The ionic mobility is function of temperature through the dynamic viscosity as $\eta = 2.761 \times$

$10^{-6} \exp(1713/T)$ [17]. To obtain local electric potential, ψ , we solve Poisson's equation by the lattice Boltzmann methods which presented in details elsewhere [45–47]. Figure 3A and B demonstrate calculated electrical conductance of two nanochannels with $H = 100$ (nm) and $H = 20$ (nm). Comparing electrical conductance of two nanochannels indicate that for high bulk ion concentration, electrical conductance versus solution temperature is independent of nanochannel height, whereas for low bulk ion concentrations, the electrical conductance could be increased (Fig. 3A) or even decreased (Fig. 3B) by increasing the solution temperature.

This behavior of electrical conductance could be interpreted by considering the overlapping of the EDLs and effects

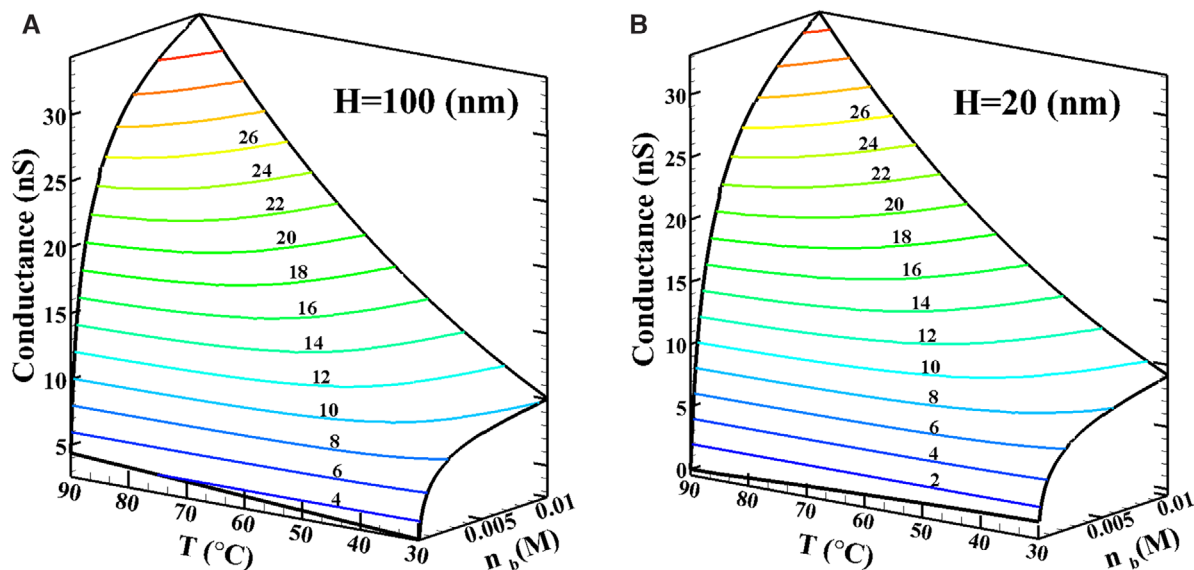


Figure 3. The calculated electrical conductance of (A) 100 (nm) and (B) 20 (nm) nanochannels versus solution temperature and bulk ion concentration.

of the flexibility of BL in response to bulk ion concentration and solution temperature in small nanochannel height.

4 Concluding remarks

In this contribution, we have investigated the effects of solution temperature on the structure of the EDL at silica-aqueous interface by proposing a new temperature dependent surface complexation model. We have shown that the interesting behavior of zeta potential as function of solution temperature and bulk ion concentration could not be solely explained by introducing the temperature dependent solid-aqueous properties to the well-known electrical triple-layer model. We found that the zeta potential behavior in response to solution temperature could be interpreted by accepting the fact that the position of ZP is not only a function of bulk ion concentration but also solution temperature. Our proposed phenomenological temperature dependent surface complexation model predicted the position of the ZP from solid surface could be increased, decreased, or even unchanged by increasing the solution temperature. Our modeling results revealed that in contrast to the zeta potential, the acquired surface charge at solid surface is always increased by increasing the solution temperature for dilute and concentrated solutions. Utilizing the proposed temperature dependent surface complexation model coupled with the Poisson–Boltzmann equation, we have obtained the electrical conductance of two distinct height nanochannels. Our calculations have demonstrated that the conductance of nanochannel versus solution temperature for concentrated solutions is independent of nanochannel height whereas, for dilute solutions, nanochannel height played a key role to determine the electrical conductance as function of solution temperature. Our

proposed phenomenological model could provide a detailed insight into the influences of solution temperature on acquired surface charge for chemically reactive surfaces and as a result, the ionic transport through micro- and nanofluidic devices.

This work is financially supported by the NSF of China (No. 51766107, 91634107) and the Tsinghua University Initiative Scientific Research Program. Our simulations are run on the “Explorer 100” cluster of Tsinghua National Laboratory for Information Science and Technology.

The authors have declared no conflict of interest.

5 References

- [1] Hunter, R. J., *Zeta Potential in Colloid Science: Principles and Applications*, 3rd ed., Academic Press, New York 1988.
- [2] Hsu, W.-L., Daiguji, H., Dunstan, D. E., Davidson, M. R., Harvie, D. J. E., *Adv. Colloid Interface Sci.* 2016, 234, 108–131.
- [3] Daiguji, H., Yang, P. D., Majumdar, A., *Nano Lett.* 2004, 4, 137–142.
- [4] Stein, D., Kruihof, M., Dekker, C., *Phys. Rev. Lett.* 2004, 93, 4.
- [5] Karnik, R., Castelino, K., Fan, R., Yang, P., Majumdar, A., *Nano Lett.* 2005, 5, 1638–1642.
- [6] Karnik, R., Fan, R., Yue, M., Li, D. Y., Yang, P. D., Majumdar, A., *Nano Lett.* 2005, 5, 943–948.
- [7] Schoch, R. B., Renaud, P., *Appl. Phys. Lett.* 2005, 86, 253111.
- [8] Alizadeh, A., Zhang, L., Wang, M., *J. Colloid Interface Sci.* 2014, 431, 50–63.

- [9] Leroy, P., Revil, A., *J. Colloid Interface Sci.* 2004, 270, 371–380.
- [10] Kitamura, A., Fujiwara, K., Yamamoto, T., Nishikawa, S., Moriyama, H., *J. Nucl. Sci. Technol.* 1999, 36, 1167–1175.
- [11] Revil, A., Glover, P. W. J., *Phys. Rev. B: Condens. Matter Mater. Phys.* 1997, 55, 1757–1773.
- [12] Revil, A., Pezard, P. A., Glover, P. W. J., *J. Geophys. Res.: Solid Earth* 1999, 104, 20021–20031.
- [13] Reppert, P. M., Morgan, F. D., *J. Geophys. Res.: Solid Earth* 2003, 108, 2546.
- [14] Lyklema, J., *Fundamentals of Interface and Colloid Science, Vol II: Solid-Liquid Interfaces*, Academic Press, London 2001.
- [15] Masliyah, J. H., S. Bhattacharjee, *Electrokinetic and Colloid Transport Phenomena*, John Wiley & Sons, New Jersey 2006.
- [16] Hunter, R. J., *Foundations of Colloid Science*, Oxford University Press, Oxford 2001.
- [17] Kim, H., Kwak, H. S., Westerweel, J., *Colloids Surf. Physicochem. Eng. Aspects* 2011, 376, 53–58.
- [18] Hsu, J.-P., Tai, Y.-H., Yeh, L.-H., Tseng, S., *Langmuir* 2012, 28, 1013–1019.
- [19] Liu, Y., Han, X., He, L., Yin, Y., *Angew. Chem., Int. Ed.* 2012, 51, 6373–6377.
- [20] Gallo-Villanueva, R. C., Sano, M. B., Lapizco-Encinas, B. H., Davalos, R. V., *Electrophoresis* 2014, 35, 352–361.
- [21] Taghipoor, M., Bertsch, A., Renaud, P., *Nanoscale* 2015, 7, 18799–18804.
- [22] Taghipoor, M., Bertsch, A., Renaud, P., *Proceedings of 2015 IEEE 15th International Conference Nanotechnol. (IEEE-Nano)* 2015, 1320–1323.
- [23] Yan, Z., Huang, X., Yang, C., *Microfluid. Nanofluid.* 2015, 18, 403–414.
- [24] Taghipoor, M., Bertsch, A., Renaud, P., *ACS Nano* 2015, 9, 4563–4571.
- [25] Taghipoor, M., Bertsch, A., Renaud, P., *Phys. Chem. Chem. Phys.* 2015, 17, 4160–4167.
- [26] Venditti, R., Xuan, X., Li, D., *Microfluid. Nanofluid.* 2006, 2, 493–499.
- [27] Hwang, J., Sekimoto, T., Hsu, W.-L., Kataoka, S., Endo, A., Daiguji, H., *Nanoscale* 2017, 9, 12068–12076.
- [28] Ishido, T., Mizutani, H., *J. Geophys. Res.* 1981, 86, 1763–1775.
- [29] Ishido, T., Mizutani, H., Baba, K., *Tectonophysics* 1983, 91, 89–104.
- [30] Tosha, T., Matsushima, N., Ishido, T., *Geophys. Res. Lett.* 2003, 30, 1295.
- [31] Reppert, P. M., Morgan, F. D., *J. Geophys. Res.: Solid Earth* 2003, 108, 2547.
- [32] Alekhin, Y. V., Sidorova, M. P., Ivanova, L. I., Lakshtanov, L. Z., *Colloid J. USSR+*. 1984, 46, 1032–1035.
- [33] Revil, A., Schwaeger, H., Cathles, L. M., Manhardt, P. D., *J. Geophys. Res.: Solid Earth* 1999, 104, 20033–20048.
- [34] Alizadeh, A., Wang, M., *J. Colloid Interface Sci.* 2019, 534, 195–204.
- [35] Alizadeh, A., Jin, X., Wang, M., *J. Geophys. Res.: Solid Earth* 2019, 124, 5387–5407.
- [36] Wang, M., Revil, A., *J. Colloid Interface Sci.* 2010, 343, 381–386.
- [37] Bourg, I. C., Lee, S. S., Fenter, P., Tournassat, C., *J. Phys. Chem. C* 2017, 121, 9402–9412.
- [38] Davis, J. A., James, R. O., Leckie, J. O., *J. Colloid Interface Sci.* 1978, 63, 480–499.
- [39] Charmas, R., Piasecki, W., *Langmuir* 1996, 12, 5458–5465.
- [40] Dietzel, M., Hardt, S., *J. Fluid Mech.* 2017, 813, 1060–1111.
- [41] Mukherjee, S., Dhar, J., DasGupta, S., Chakraborty, S., *Proc. R. Soc. A* 2019, 475, 20180522.
- [42] Zhang, W., Wang, Q., Zeng, M., Zhao, C., *Int. J. Heat Mass Transfer* 2019, 143, 118569.
- [43] Yang, Y., Wang, M., *J. Colloid Interface Sci.* 2018, 514, 443–451.
- [44] Yang, Y., Wang, M., *Environ. Sci. Technol.* 2019, 53, 1976–1984.
- [45] Alizadeh, A., Warkiani, M. E., Wang, M., *Microfluid. Nanofluid.* 2017, 21, 52.
- [46] Wang, J. K., Wang, M., Li, Z. X., *J. Colloid Interface Sci.* 2006, 296, 729–736.
- [47] Alizadeh, A., Wang, M., *Electrophoresis* 2017, 38, 580–595.